Numerical Study Of Heat Transfer In Cooling Passages Of Turbine Blade

Dr. Ahmed F. Khudheyer
Mech. Eng. Dept.
Al- Nahrain University
Baghdad, Iraq
ahyaja@yahoo.com

Hussein T. Dhaiban
Mech. Eng. Dept.
Al- Nahrain University
Baghdad, Iraq
huso0ony@yahoo.com

ABSTRACT

As the temperature of combustion gases is higher than the melting temperature of the turbine materials, cooling of turbine parts in a gas turbine engine is necessary for safe operation. Cooling methods investigated in this computational study included cooling flow losses. Film-cooling is one typically used cooling method whereby coolant is supplied through holes passage, in present study the holes placed along the camber line of the blade.

The subject of this paper is to evaluate the heat transfer that occur on the holes of blade through different blowing coolant rates. The cases of this study were performed in a low speed wind tunnel with two tip gap at small and large (0.03 and 0.09cm) and multiple coolant flow rates through the film-cooling holes. The blowing ratios was studied whereby coolant was injected from holes placed along the tip of a large scale blade model with Reynolds number (2.1×10^5) of the engine was matched. Results showed that baseline Nusselt numbers on the holes were reduced along the holes passage, and heat transfer coefficient is high values at iterance region. Overall, the cooling by holes appears to be a feasible method for prolonging blade life.

KEYWORDS: heat and mass transfer, gas turbine cooling

الخلاصة:

درجة حرارة غازاتِ الاحتراق تكون عالية بالمقارنة مع درجةِ حرارة ذَوَبان معادن التوربين، تَبريد أجزاء التوربين في محرّك التوربين الغازي ضروريُة لعمله في ظروف أمنة. نظريات التبريد تحققت في الدراسة النظرية بحيث تضمنت خسائر جريان التبريد. التبريد الغشائي (film-cooling) هو احد طرق التبريد النموذجية حيث أن مائع التبريد يجهز من خلال الثقوب، في الدراسة الحالية تقع الثقوب على طول خط المنتصف (camber) لريشة التوربين.

هدف هذا البحث هو حساب انتقال الحرارة الذي يحدث داخل ثقوب الريشة من خلال نسب تبريد متغيرة. حالات الدراسة أنجزت على جريان بطيء في النفق الهوائي مع فجوتان للقمة صغيرة وكبيرة (0.03 و 0.09 سم) مع اختلاف نسب مائع التبريد من خلال ثقوب التبريد الغشائي (film-cooling). تم دارسة Blowing Ratios من خلال جريان مائع التبريد الذي يحقن من الثقوب التي تقع على طول القمة مع مقياس كبير لنموذج الريشة مع رقم رينولد ($2.1 * 10^5$) للمحرك الذي يكون محسوب. النتائج توضح أرقام نسلت في الثقوب تقل على طول الثقوب، ومعامل انتقال الحرارة يكون ذو قيمة عالية عند منطقة الدخول. عموماً، التبريد بواسطة الفتحات تَبْدو طريقة ملائمة لإطالة عمر الريشة.

INTRODUCTION

Gas turbine engines are widely used to power aircraft because they are light and compact and have a high power to-weight ratio. One way to increase power and efficiency of gas turbines is

by increasing turbine-operating temperatures. The motivation behind this is that higher temperature gases yield higher energy potential. However, the components along the hot gas path experience high thermal loading, which can cause distress. The HPT (High Pressure Turbine) first stage blade is one component that is extremely vulnerable to the hot gas**.**

The two main objectives of blade design engineers are (1) to reduce the leakage flow either by reducing the tip gap or by implementing a more effective tip leakage sealing mechanism and (2) to cool the blade tips with the least possible usage of cooling fluid, Bunker, (2002).

The degree of cooling which may be achieved is dependent upon a number of factors, chief among which are (a) the temperature difference between the main gas stream and the inlet cooling air and (b) the 'conductance ratio', this being defined as the ratio of the heat input to the blade per unit temperature difference between gas stream and blade to the heat passed to the cooling air per unit temperature difference between blade and cooling air, Nasir et al. (2003).

Clearly to achieve a high degree of cooling the lowest possible value of conductance ratio is required in conjunction with the largest possible temperature difference between gas stream and cooling air. The heat input to the blade per unit temperature difference between gas stream and blade is the product of the average gas-to-blade heat transfer coefficient and the external surface area, and this in turn is dependent upon the blade shape, gas flow incidence, gas flow Reynolds number, gas Prandtl number, and to a lesser extent upon the ratio of gas temperature to blade temperature, and also gas stream Mach number, Jonas (2002).

The cooling air is forced through a porous blade wall. This method is by far the most economical in cooling air, because not only it remove heat from the wall more uniformly, but the effusion layer of air insulates the outer surface from the hot gas stream and so reduces the rate of heat transfer to the blade, Cohen (1987)**.**

Gas turbine blades usually have a gap between the blade tip and the stationary casing or the shroud surface known as tip gap. This clearance gap is necessary to allow for the blade's mechanical and thermal growth. The leakage flow (flow through the tip gap) results in a reduction in the blade force, the work done and therefore the efficiency. Fig. (1) shows the gap between the blade and shroud**,** Allen and Kofskey (1955).

Allen and Kofskey (1955) performed some visualization tests to see what these secondary flows looked like. Additionally, they also studied the effect of ejecting flow from the turbine tips on the shape of the secondary flows. At the time of these tests, engine temperatures were not so high as to require cooling of the turbine blades for operation but they noted that, "turbine blade cooling may become an engine requisite. The turbine rotor blade cooling method of passing cooling air through hollow blades and discharging it at the blade tip may be one of the most feasible methods of changing the secondary-flow pattern".

Yang et al. (2004) predicted film cooling effectiveness and heat transfer coefficient for three types of film-hole arrangements: 1) the holes located on the mid-camber line of the tips, 2) the holes located upstream of the tip leakage flow and high heat transfer region, 3) combined arrangements of camber and upstream holes. They found that upstream film hole arrangements provided better film cooling performance than camber arrangements.

Acharya et al. (2003) indicated that film cooling injection lowered the local pressure ratio and altered the nature of the leakage vortex. High film-adiabatic effectiveness and low heat transfer coefficients were predicted along the coolant trajectory with the lateral spreading of the coolant jets being quite small for all cases. With an increased tip gap the coolant was able to provide better downstream effectiveness through increased mixing. For the smallest tip gap, the coolant was shown to impinge directly on the surface of the shroud leading to high film effectiveness at the impingement point. As the gap size increased, their predictions indicated that

the coolant jets were unable to penetrate to the shroud.

Nasir et al. (2003) found that a single squealer on the suction side performed the test. The performance of different recessed tip geometries were investigated and compared with plane tip performance. A transient liquid crystal technique was employed to measure detailed heat transfer coefficient distributions. Coolant injection from holes located on the blade tip, near the tip along the pressure side and combination cases were also investigated. Experiments were performed for plane tip and squealer tip for different coolant to mainstream blowing ratios of 1.0, 2.0, and 3.0. A transient infrared (IR) thermography technique was used to simultaneously measure heat transfer coefficient and film cooling effectiveness. He shows the tip injection reduced heat transfer coefficient on the blade tip and an increase in blowing ratio caused a decrease in heat transfer coefficient for both plane and squealer tip blade.

Christophel et al. (2004) evaluated the adiabatic effectiveness levels that occur on the blade tip through blowing coolant from holes placed near the tip of a blade along the pressure side. Also present were dirt purge holes on the blade tip, which is part of a commonly used blade design to expel any large particles present in the coolant stream. Experiments were conducted in a linear cascade with a scaled-up turbine blade, from these tests indicated that the performance of cooling holes placed along the pressure side tip was better for a small tip gap than for a large tip gap. Disregarding the area cooled by the dirt purge holes, for a small tip gap the cooling holes provided relatively good coverage. For all of the cases considered, the cooling pattern was quite streaky in nature, indicating very little spreading of the jets. As the blowing ratio was increased for the small tip gap, there was an increase in the local effectiveness levels resulting in higher maxima and minima of effectiveness along the middle of the blade.

Hohlfeld et al. (2003) investigated in this computational study included cooling flow losses and microcircuit channels. This study evaluated the benefit of external film-cooling flow exhausted from strategically placed microcircuits. Along the blade tip, predictions showed mid-chord cooling was independent of the blowing from microcircuit exits. The formation of a pressure side vortex was found to develop for most microcircuit film-cooling cases. Significant leading edge cooling was obtained from coolant exiting from dirt purge holes with a small tip gap while little cooling was seen with a large tip gap.

Couch (2003) studied examinations of a novel cooling technique called a microcircuit, which combines internal convection and pressure side injection on a turbine blade tip. Holes on the tip called dirt purge holes expel dirt from the blade, so other holes are not clogged. Wind tunnel tests were used to observe how effectively dirt purge and microcircuit designs cool the tip. Tip gap size and blowing ratio are varied for different tip cooling configurations. Results show that the dirt purge holes provide significant film cooling on the leading edge with a small tip gap. Coolant injected from these holes impacts the shroud and floods the tip gap reducing tip leakage flow. Also, results suggest that blowing from the microcircuit diminishes the tip leakage vortex.

The objectives of the work presented in this paper are to present the benefits of heat transfer of a holes using coolant exhausted from holes to tip at different blowing ratio.

NUMERICAL ANALYSIS

The basic equations that describe the flow and heat are conservation of mass, momentum and energy equations. These equations describe two-dimensional, turbulent and incompressible flow takes which the following forms: (Arnal, M.P,1982):

The assumptions that used for the instantaneous equation are:-

1- Steady, two-dimensional, incompressible flow, single phase flow, shock free, inviscous, no slip, irrotational.
2- The fluid is Newtonian.
3- Cylindrical coordinate for flow in cooling passages.

(i) *Conservation of Mass*

$$\frac{\partial}{\partial z}(\rho u) + \frac{1}{r}\frac{\partial}{\partial r}(\rho r v) = 0 \qquad (1)$$

(ii) *Momentum Equations*

u-momentum (z-direction)

$$\frac{1}{r}\left[\frac{\partial}{\partial z}(\rho ruu)+\frac{\partial}{\partial r}(\rho ruv)\right]=-\frac{\partial p}{\partial z}+\frac{1}{r}\left[\frac{\partial}{\partial z}\left(r\mu_{eff}\frac{\partial u}{\partial z}\right)+\frac{\partial}{\partial r}\left(r\mu_{eff}\frac{\partial u}{\partial r}\right)\right]+S_u \quad (2)$$

v-momentum (r-direction)

$$\frac{1}{r}\left[\frac{\partial}{\partial z}(\rho ruv)+\frac{\partial}{\partial r}(\rho rvv)\right]=-\frac{\partial p}{\partial r}+\frac{1}{r}\left[\frac{\partial}{\partial z}\left(r\mu_{eff}\frac{\partial v}{\partial z}\right)+\frac{\partial}{\partial r}\left(r\mu_{eff}\frac{\partial v}{\partial r}\right)-\Gamma^v\frac{v}{r^2}\right]+S_v \quad (3)$$

(iii) *Energy Equation*

$$\frac{1}{r}\left[\frac{\partial}{\partial z}(\rho ruT)+\frac{\partial}{\partial r}(\rho rvT)\right]=\frac{1}{r}\left[\frac{\partial}{\partial z}\left(r\Gamma_{eff}\frac{\partial T}{\partial z}\right)+\frac{\partial}{\partial r}\left(r\Gamma_{eff}\frac{\partial T}{\partial r}\right)\right] \quad (4)$$

The turbulence model utilized in this analysis is the two equation k-Epsilon model. This model is utilized for its proven accuracy in turbine blade analysis and for its applicability to confined fluid flow. (k- ε) Turbulence Model is one of the most widely used turbulence models is the two-equation model of kinetic energy (k) and its dissipation rate (**ε**). The turbulence according to Launder and Spalding (1972) is assumed to be characterized by its kinetic energy and dissipation rate (**ε**), where

(i) *Turbulence Energy, k*

$$\frac{1}{r}\left[\frac{\partial}{\partial z}(\rho ruk)+\frac{\partial}{\partial r}(\rho rvk)\right]=\frac{1}{r}\left[\frac{\partial}{\partial z}\left(r\Gamma^k\frac{\partial k}{\partial z}\right)+\frac{\partial}{\partial r}\left(r\Gamma^k\frac{\partial k}{\partial r}\right)+G-\rho\varepsilon\right] \quad (5)$$

(ii) *Energy Dissipation Rate, ε*

$$\frac{1}{r}\left[\frac{\partial}{\partial z}(\rho ru\varepsilon)+\frac{\partial}{\partial r}(\rho rv\varepsilon)\right]=\frac{1}{r}\left[\frac{\partial}{\partial z}\left(r\Gamma^\varepsilon\frac{\partial \varepsilon}{\partial z}\right)+\frac{\partial}{\partial r}\left(r\Gamma^\varepsilon\frac{\partial \varepsilon}{\partial r}\right)\right]+c_1\frac{\varepsilon}{k}G-c_2\rho\frac{\varepsilon^2}{k} \quad (6)$$

where

$$G=\mu_t\left\{2\left[\left(\frac{\partial u}{\partial z}\right)^2+\left(\frac{\partial v}{\partial r}\right)^2+\left(\frac{v}{r}\right)^2\right]+\left(\frac{\partial u}{\partial z}+\frac{\partial v}{\partial r}\right)^2\right\}+S_G \quad (7)$$

given by (Ideriah, F. J. K.,1975)

$$S_G=-\frac{2}{3}\mu_t\left[\frac{\partial u}{\partial z}+\frac{\partial v}{\partial r}\right]^2-\frac{2}{3}\rho k\left[\frac{\partial u}{\partial z}+\frac{\partial v}{\partial r}\right] \quad (8)$$

The values of the empirical constant used here are given in Table (1). (Launder and Spalding,1974) **[11]**.

The governing equations (1),(2),(3),(4),(5) and (6) can be write in one general form as shown below:

$$\frac{\partial(\rho u\phi)}{\partial z}+\frac{1}{r}\frac{\partial(\rho rv\phi)}{\partial r}=\frac{\partial}{\partial z}\left(\Gamma^\phi\frac{\partial\phi}{\partial z}\right)+\frac{1}{r}\frac{\partial}{\partial r}\left(r\Gamma^\phi\frac{\partial\phi}{\partial r}\right)+S_\phi \quad (10)$$

where :-

(ø) is any dependent variable.

(Γ^ϕ) is any exchange coefficient of ø.

($S_ø$) is the source term of ø.

The transform equation (10) from physical domain to computational domain, and that lead to obtained the transformation of the governing equations as follows:-

$$\frac{\partial}{\partial\zeta}(\rho\phi G_1)+\frac{\partial}{\partial\eta}(\rho\phi G_2)=\frac{\partial}{\partial\zeta}\left(\Gamma^\phi Ja\frac{\partial\phi}{\partial\zeta}\right)+\frac{\partial}{\partial\eta}\left(\Gamma^\phi Jc\frac{\partial\phi}{\partial\eta}\right)+S_{total} \quad (11)$$

where:-

G_1 and G_2 are the contravariant velocities or the mass flow rates in the ζ and η direction respectively. Also (a, b and c) are the transformation coefficient to computational domain and S_{total} is the total source terms.

The governing equations are integrated over each control volume (C.V.) with each its neighbor nodes. This discretization of the steady, 2-D governing equations is done by using finite volume method with collocated grid arrangement by using the upwind differencing scheme. Also discretization the terms of source term to give the solving the governing equations.

After solving the momentum equation, the velocity field obtained does not guarantee the conservation of mass unless the pressure field is correct, therefore, the velocity component (u, v), (G_1,G_2), pressure must be corrected according to the continuity equation, (Karki and Patankar, 1989)[13].

In the present work, the (SIMPLE) algorithm (**S**emi-**I**mplicit **M**ethod for **P**ressure

$$\text{Also, } \mu_t = \rho c_\mu k^2 / \varepsilon \qquad (9)$$

Linked **E**quation) is used to couple the pressure and velocity as in (Veresteeg & Malalasekera, 1995). This method is done by solving the momentum equations using the guessed pressure field to obtain the velocity then, the velocity field that obtained satisfies the momentum equations, then the velocity and pressure are corrected because the velocity field violates the conservation of mass.

GEOMETRY OF FLOW AND BOUNDARY CONDITIONS

A Three-dimensional blade profile was created for these low speed. The scaling and design of blade profile and duct are discussed in Hohlfeld (2003)**.** Table (2) lists the run conditions and input to the numerical simulations. The boundary condition on a blade surface assumes zero relative velocity between the blade surface and the shroud. All walls were adiabatic for adiabatic effectiveness cases. The main inlet was specified as a constant velocity inlet at **11.3** m/s. The inlet temperature in the duct (T_g) is 750 □C (taken from al-Dorah power station), the temperature that is used in cooling (T_c) take at 27 □C and the pressure that used at atmosphere condition. The cooling holes locations is shown in Tables (3). The coordinate system was adjusted so that no coordinates are negative**.**

COMPUTATIONAL METHOLOGY

Computational fluid dynamics (CFD) simulation is performed to analyze the heat transfer in holes. A commercially available CFD code, Fluent 6.3.26 (2009) was used to perform all simulations. Fluent is a pressure based flow solver that can be used with structured or unstructured grids. An unstructured grid was used for the study presented in this paper. Solutions were obtained by numerically solving the Navier-Stokes and energy equation through a control volume technique. All geometric construction and meshing were performed with GAMBIT 2.4.6.

To ensure a high quality mesh, the flow passage was divided into multiple volumes, which allowed for more control during meshing. The tip gap region was of primary concern and was composed entirely of tetrahedral cells. Inlet conditions to the model were set as a uniform inlet velocity at approximately one chord upstream of the blade. Fig. (2) shows the mesh of the test rig. An inlet mass flow boundary condition was imposed for the coolant at the plenum entrance for the cooling holes. The mesh contained approximately 20 grid points across the hole exit. Mainstream flow angles were set to those of the experiments as well as the scaled values for the engine while the turbulence intensity and mixing length were set to 4.3% and 0.3 m, respectively.

To allow for reasonable computational times, all computations were performed using the RNG k-ε turbulence model with non-equilibrium wall functions whereby the near wall region was resolved to y^+ values ranging between 30 and 60. Mesh insensitivity was confirmed through several grid adaption based on viscous wall values, velocity gradients, and temperature gradients. Typical mesh sizes were composed of 4.8 million cells with 40% of the cells in and around the tip gap region. Typical computations required 2000 iterations for convergence.

HEAT TRANSFER CALCULATION

In the present study, the numerically measured mass flow rates and air exit temperatures for all cooling passages where used to calculate the total heat transfer is:

$$Q = \square\ Cp\ (T_e - T_{in}) \qquad (12)$$

where T_{in} is the cold temperature, T_e is the exit temperature from hole passage.

After that comparison is made between total heat transfer and heat transfer by convection in holes to find local heat transfer coefficient, which will be used to calculate local Nusselt number for different walls of the holes passages.

$$Nu_x = \frac{h_x d}{k} \quad (13)$$

where h_x is the local heat transfer coefficient, d is the diameter of pipe.

Next the average heat transfer coefficient for the cold side is found by averaging the heat transfer coefficients predicted by Dittus-Boelter correlation for each hole:

$$Nu = 0.023 (Re_{pipe})^n (Pr)^s \quad (14)$$

where n=0.8, s= 0.4 (heating flow)

The summery of present study is presented in Table (4)

RESULS AND DISCUSSION

Results are shown for cases with a baseline flat tip and coolant injection at a small and large tip gap (0.03 and 0.09 cm) respectively. Blowing ratio is the ratio between velocity at mainstream condition to velocity at cooling condition at constant density (BR= U_∞/U_c). In present study, the blowing ratios of 0.5%, 1%, 1.5% and 2% are studied.

Fig. (3) shows the pressure distribution around the blade at midspan for small tip gap in suction and pressure side with the pressure non-dimensionalized by the inlet pressure conditions and given in C_p parameters. Also this results comparison with experimental and computational data for Christophel et al (2004). When the air approaching the leading edge of a blade is first slowed down, it then speeds up again as it passes over or beneath the blade. As the velocity changes, so does the dynamic pressure and static pressure according to Bernoulli's principle. Air near the stagnation point has slowed down, and thus the static pressure in this region is higher than the inlet static pressure to main duct. Air that is passing above and below the blade, and thus has speeded up to a value higher than the main inlet path velocity, will produce static pressures that are lower than inlet static pressure. At a point near maximum thickness, maximum velocity and minimum static pressure will occur. Also this figure shows a good agreement with the experimental and computational data for Christophel et al..

Fig. (4) indicates the wall temperature distribution of the air flow through the holes passages and relation with the dimensionless distance of span (z/s). This figure shows hole 10 is at high temperature because the small distance between the suction and pressure side and high temperature at this region, also shows the hole 1 is high wall temperature because the effect of mainstream flow is high at leading edge region. Additionally, this figure shows the low temperature at hole 3 and hole 4 because maximum distance between suction and pressure and the high temperature at the surface does not affect largely on these holes. From Fig. (4), the wall temperature has minimum values (temperature of air) at zero dimensional horizontal z (at entrance region), and maximum values at the end of dimensional distance because of the mixing between cooled and high temperature, also shows stability in temperatures at mid of holes from (z/s=0.2 to z/s=0.8).

Fig. (5) shows the laterally averaged adiabatic effectiveness for small tip gap of the air flow through the holes passages and shows the relation between effectiveness and dimensionless distance of span (z/s). The effectiveness at zero dimensional is high value because the start of cooling happens, but at end of dimensionless distance (z/s) has low effectiveness because of mixing the cooled flow with hot mainstream. Additionally, this figure shows hole 10 has low effectiveness and hole 4 has high effectiveness.

Fig. (6) indicates the local heat transfer coefficient (h) in holes passages with small tip gap, and the relation between (h) and dimensionless distance of span (z/s). This figure shows the local heat transfer coefficient is stable at large range of dimension from (0.2 to 0.8), and decreases at the end of dimensionless distance (z/s), because the large temperature difference between the flow and wall. Additionally heat transfer coefficient at zero dimensionless (z/s) is very large because of low temperature difference between the surface and main temperature of the flow pipe.

Fig. (7) indicates the local Nusselt number distribution at the holes passages and relation with the dimensionless distance of span (z/s). This figure shows high value of Nusselt number in the region before (z/s=0.2) because of high value of local heat transfer coefficient and low value of temperature difference between the

pipe surface and flow inside it, it also shows stable values for the range of (0.2<z/s<0.8) and decrease at the end of dimensionless. Also, hole 1 and hole 10 have minimum Nusselt number and hole 4 has maximum Nusselt number. Also **Fig. (8)** shows the dimensionless Nusselt number relates with dimensionless distance of span (z/s) at small tip gap, when the dimensionless Nusselt is calculated by dividing local Nusselt number to average Nusselt number from Dittus-Boelter correlation. Results show the dimensionless Nusselt number has the same behavior of Fig. (6).

Fig. (9) indicates the average Nusselt number in all holes related with dimensionless distance of span. Twenty points from each segment are chosen and the average point in all hole is found, the equation representing Nusselt number using polynomial with ten degrees of curve fitting which is applied by Tecplot software computer program for drawings. This figure shows high value of Nusselt number at enterance region of dimensionless and low value at the end of diamensionless and shows the Nusselt is nearly stable at mid for the range of (0.2<z/s<0.8) at fully developed region.

*All figures take at small tip gap with blowing ratio at (1%), but in large tip gap is not different large in small tip gap only at exit of holes or at end of dimensionless when high temperature at this region because high leakage flow enter that mean high hot mainstream is entered to this region of mixing***.**

Fig. (10) indicates the relation between dimensionless Nusselt number with the dimensionless distance of span (z/s) at different blowing ratios of small tip gap at hole 1. **Hole 1** is the hot hole between all holes of blade. This figure shows low dimensionless Nusselt number at low blowing ratio and this value increases with increasing the blowing ratio, but that is limited, dimensionless Nusselt number of blowing ratio at 2% is lowest value of dimensionless Nusselt number of blowing ratio of 1.5%. When talk about small tip gap the coolant flow that exit from hole 1 at different blowing ratio is impact at shroud and mixed with the leakage flow and this mixing is not affected of high blowing ratio at 2% because when the velocity of hole passage increases, it impacts the shroud and some of the flow will be dissipated, therefore any increasing in coolant flow is dissipated also.

Fig. (11) indicates the relation between dimensionless Nusselt number with the dimensionless distance of span (z/s) at different blowing ratios of small tip gap at hole 4. **Hole 4** is the cold hole between all holes of blade. This figure shows that the Nusselt number is decreased along the hole which is verified with the temperature distribution behaviors, and shows low dimensionless Nusselt number at low blowing ratio at 0.5% and this value increases with increasing the blowing ratio to 1%, but that is limited also, dimensionless Nusselt number of high blowing ratios at 1.5% and 2% are lowest values of dimensionless Nusselt number of low blowing ratios at 0.5% and 1%, because the coolant flow impacts the shroud and makes the flow inside pipe slow, and notes the coolant flow is poor mixed with the leakage flow, therefore that makes the high blowing ratio decrease.

CONCLUSION

From the results, it can be concluded that the heat transfer can reach the max value at the hole of the number 4 (at maximum distance of blade) and min value at the hole of numbers 1 (when flow was impact at the blade at leading edge) and 10 (at minimum distance at trailing edge) [the number of holes shows in Fig.(2-b)]. Heat transfer coefficient is high values at entrance regions. Results showed that baseline Nusselt numbers on the holes were reduced along the holes. The cooling of blade increases as the amount of blowing ratio increases but that is limited because the flow will be dissipated**.** Finally, the pressure coefficient distribution is same in engine when compared with experimental data of Christophel et al. (2004).

Nomenclature

Symbol	*Description*	Dimension
A	Coefficient of the discretized equation, area	m^2
B_x	Axial chord of the blade	m
C	Chord of the blade	m
G_1,G_2	Contravariant velocity in ξ,η, respectively	m/s
J	Jacobian of coordinates transformation	
P	Pressure	pa
Re_{pipe}	Reynolds Number (Re=ρUD/μ)	
Nu	Nusselt number (hd/k)	
S	Span length	m
$S_{\square}$	Source term of □	
T	Temperature	K
u ,v	Velocity component in r, z respectively	m/s
U_∞	Velocity at mainstream conditions	m/s
U_c	Velocity at cooling condition	m/s
BR	Blowing ratio(U_∞/ U_c)	
P	Static pressure	N/m^2
T_g	Temperature of hot gases	□ C
T_c	Temperature of cooling air	□ C
T_{in}	Temperature at inlet condition	□ C
u, v	Velocity component in x ,y coordinate direction respectively	m/s
r,z	Cylindrical coordinate	
	Subscript	
ξ ,η	Partial derivative in the computational plane	
aw	Adiabatic wall	
	Superscript	
c	Coolant conditions	
∞	Mainstream conditions	
	Greek Letters	
□	Dependent variable	
η	Adiabatic effectiveness , $\eta = (T_{in}-T_{aw})/(T_{in}-T_c)$	
C_p	$(p - p_{in})/(0.5\,\rho\, U_{in}^2)$	
ρ	Density	kg/
ε	Rate of dissipation of kinetic energy	m^2
μ	Dynamic viscosity	N.n

	Abbreviation
C.F.D	Computational Fluid Dynamics
SIMPLE	Semi-Implicit Method for Pressure Linked Equation

REFRENCES

Acharya, S., Yonk, H., Prakash, C. and Bunker, R., "Numerical Study of Flow and Heat Transfer on a Blade tip with Different Leakage Reduction Strategies", ASME paper No. GT-2003-38617, 2003.

Allen, H. W. and. Kofskey, M.G, "Visualization Study of Secondary Flows in Turbine Rotor Tip Regions", NACA Technical Note 3519, 1955.

Arnal, M.P., "A General computer program for two-dimensional, turbulent, re-circulating flows", Report No.Fm-83-2, 1983.

Bunker, R. S., "Cooling Design Analysis", AIAA Journal of Propulsion and Power, 2002.

Christophel, J. R., Couch, E., Thole, K. A. and Cunha, F. J., "Measured Adiabatic Effectiveness and Heat Transfer for Blowing from the Tip of a Turbine Blade", ASME paper No. GT2004-53250, 2004.

Cohen H., Rogers G.F.C., and Saravanamutto H.I.H., "Gas turbine theory", 3rd edition, Longman scientific and technical, 1987.

Couch, E., "Measurement of Cooling Effectiveness along the Tip of a Turbine Blade", Master's Thesis, Virginia Polytechnic Institute and State University, Blacksburg, VA, 2003.

Fluent Inc., Fluent User's Guide, Version 6.3.26, 2009.

Hohlfeld, E. M., "Film Cooling Predictions Alone the Tip and Platform of a Turbine Blade",

Master's Thesis, Virginia Polytechnic Institute and State University, Blacksburg, VA, 2003.

Ideriah, F. J. K., "Review of equation solved in TEACH", private communication, 1975

Jonas, B., "Internal cooling of gas turbine blades", PhD, Chalmers university of Technology Goterborg, Sweden, 2002.

Karki, K., and Patankar, S., "Pressure Based Calculation Procedure for Viscous Flows at All Speeds in Arbitrary Configurations", ALAa Journal, Vol. 27, PP. 1167-1174, 1989.

Launder, B.E. and Spalding, D.B.," Mathematical models of turbulence", Academic press, London, 1972.

Nasir H. S., Ekkad, V., Divad M. K., Bunker, R. S. and Prakash C., "Effect of Tip Gap and Squealer Geometry on Measured Heat Transfer Over a HPT Rotor Blade Tip", J. of Turbomachinery, 125, pp. 221-228, 2003.

Verestage, H. K., and Malalasekera, W., "An Introduction to Computational Fluid Dynamic-The Finite volume Method", Longman Group Ltd, 1995.

Yang, H., Chen, H-C and Han, J-C, "Numerical Prediction of Film Cooling and Heat Transfer With Different Hole Arrangements on the plane and Squealer Tip of a Gas Turbine Blade", ASME Paper No. GT2004-53199, 2004.

Table (1) Values of constants in the (k-ε) model.

C_μ	C_D	C_1	C_2	σ_k	σ_ε
0.09	**1.0**	**1.44**	**1.92**	**1.0**	**1.3**

Table (2) Special design of geometry and flow condition of the blade from Hohlfeld (2003).

Parameter	Value
Scaling Factor	12X
Axial Chord, B_x	35 cm
True Chord, C	53 cm
Pitch, P	43 cm
Span, S	55.2 cm
Re	2.1E+05
Inlet Angle, θ	16.5°
Blade Angle, □	50□
Small tip gap, h	0.03 cm
Large tip gap, H	0.09 c m

Table (3) Holes locations.

Holes	X(cm)	Y(cm)	Diameter(cm)
1	3.43	40.5	0.7
2	6.86	40.43	0.7
3	10.3	39.5	0.7
4	13.7	37.68	0.6
5	17.15	34.91	0.6
6	20.3	31.48	0.6
7	23.2	27.15	0.6
8	26.02	21.857	0.6
9	28.45	16.802	0.6
10	30.88	10.66	0.6

Table (4) Summery of present study

Governing equations	Continuity, Navair-Stokes, Energy, Turbulent Kinetic Energy and dissipation rate
Coordinates	Non-Orthogonal body fitted coordinate system
Assumptions	Perfect gas, steady, incompressible, single phase, shock free, turbulent
Grid generation	Algebraic equations
Transformation from physical to computational domain	Jacopian
General form of discretization	Finite volume
Grid arrangement	Collocated
Convective Schemes	Upwind
Pressure-velocity coupling	SIMLPE algorithm
Matrix solution method	TDME
Boundary condition	**1.** No-slip condition was applied to the shroud and all blade surfaces. **2.** All walls were adiabatic for adiabatic effectiveness cases, and for heat transfer coefficient cases only the tip or tip and shelf were changed to have constant heat flux conditions. **3.** The main inlet was specified as a constant velocity inlet at **11.3** m/s .

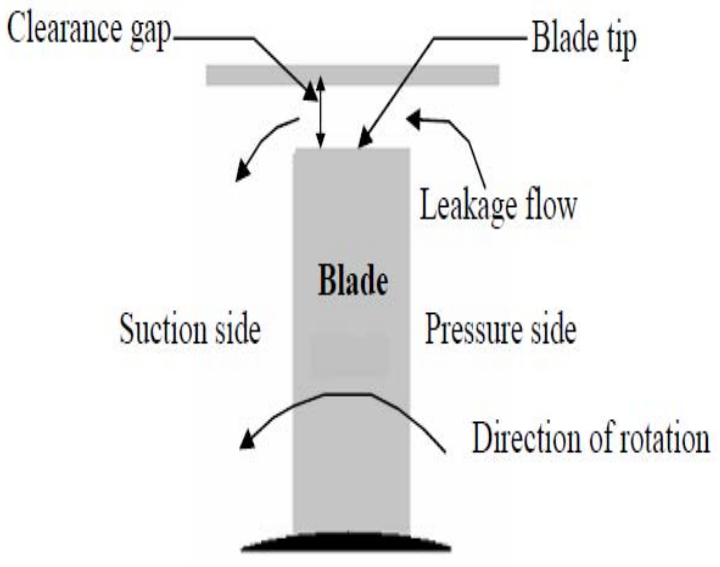

Fig. (1) Conceptual view of the leakage flow through the clearance gap.

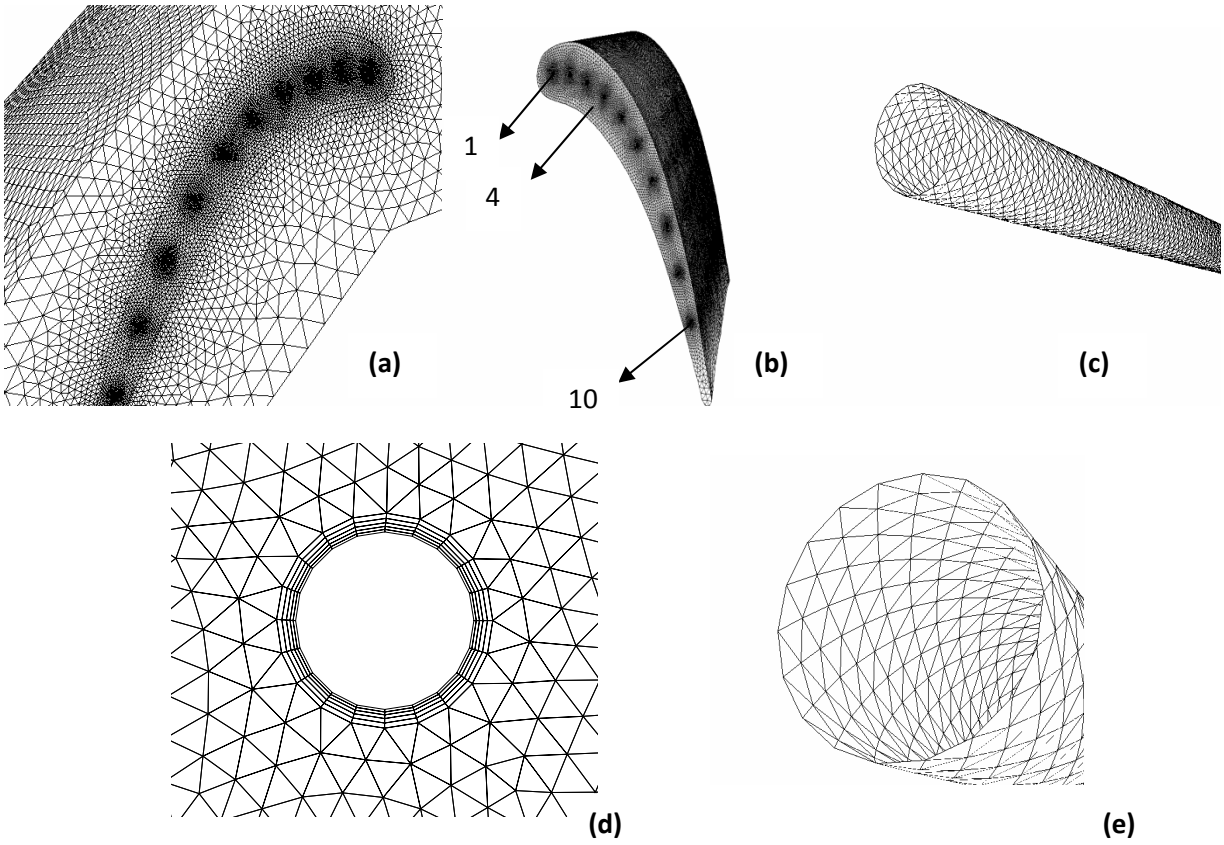

Fig. (2) Shows the mesh at (a) duct, (b) blade, (c) holes, (d) boundary layer around the holes and (e) point at holes edge.

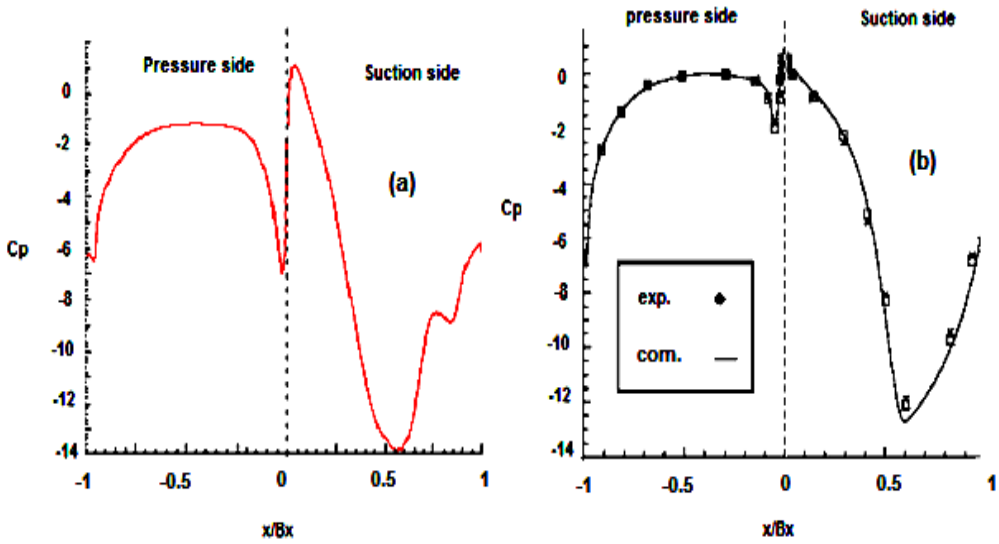

Fig. (3) Predicted static pressure distributions at suction and pressure side for (a) computational of present study, (b) experimental and computational from Christophel et al (2004).

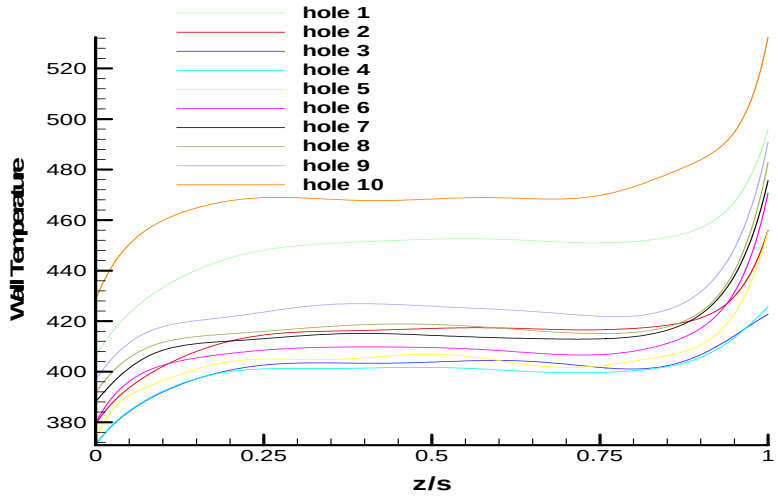

Fig. (4) The wall temperature distribution through the length of holes in small tip gap.

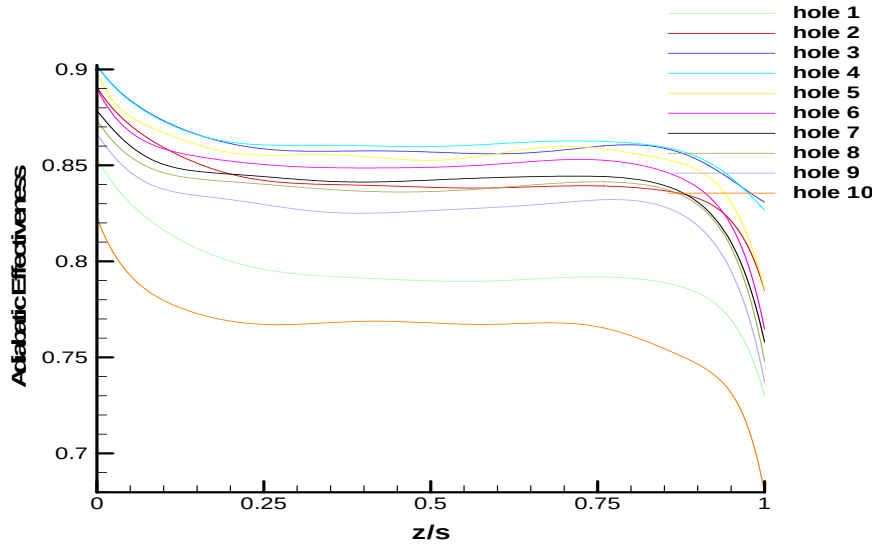

Fig. (5) Laterally averaged adiabatic effectiveness alone the holes at small tip gap.

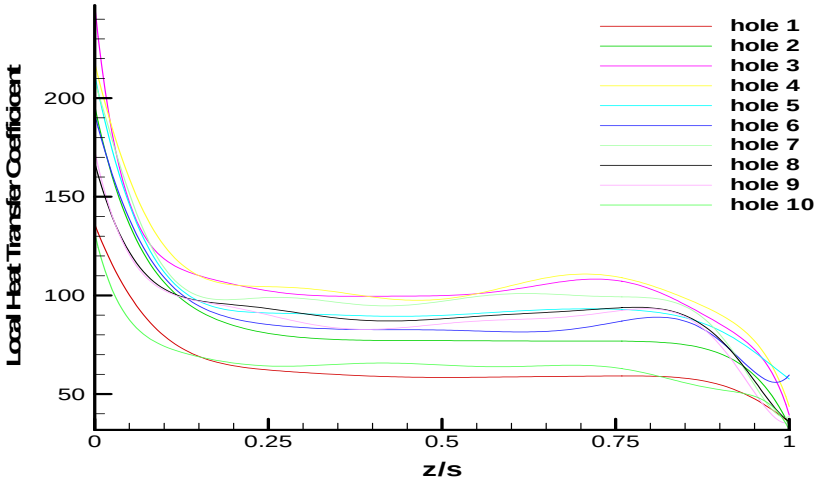

Fig. (6) Local heat transfer coefficient alone the holes at small tip gap.

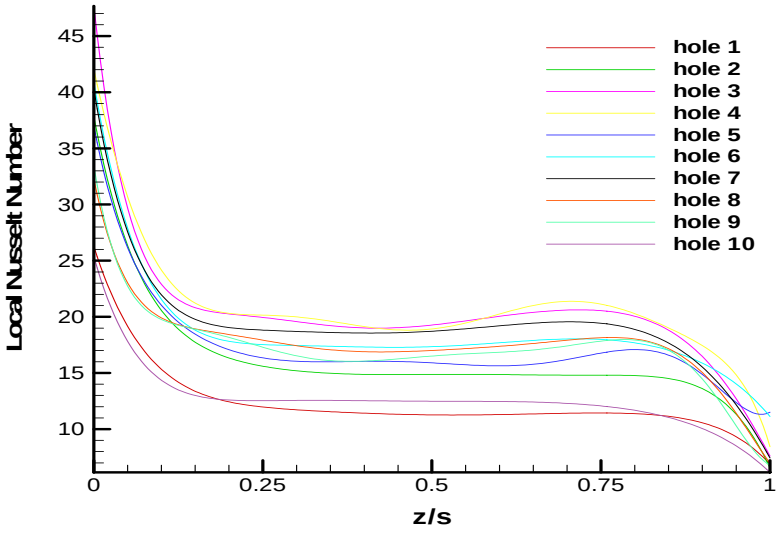

Fig. (7) Local Nusselt Number alone the holes at small tip gap.

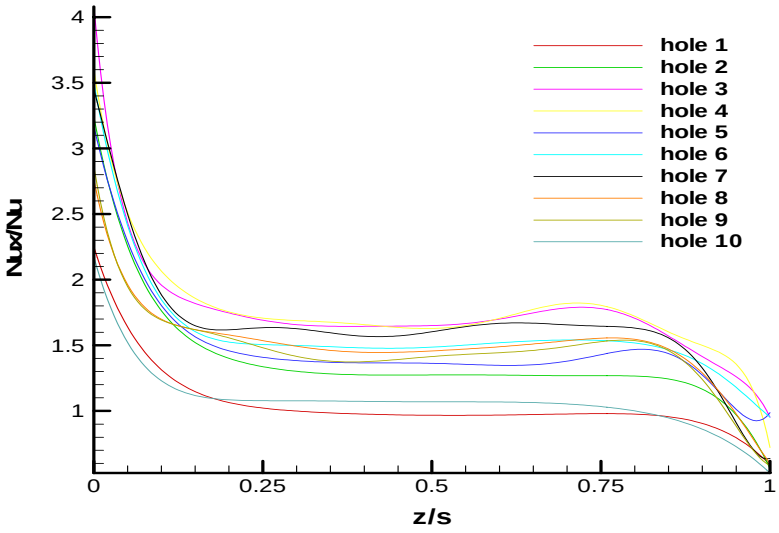

Fig. (8) The Relation between dimensionless Nusselt number and distance of span at different holes of blade.

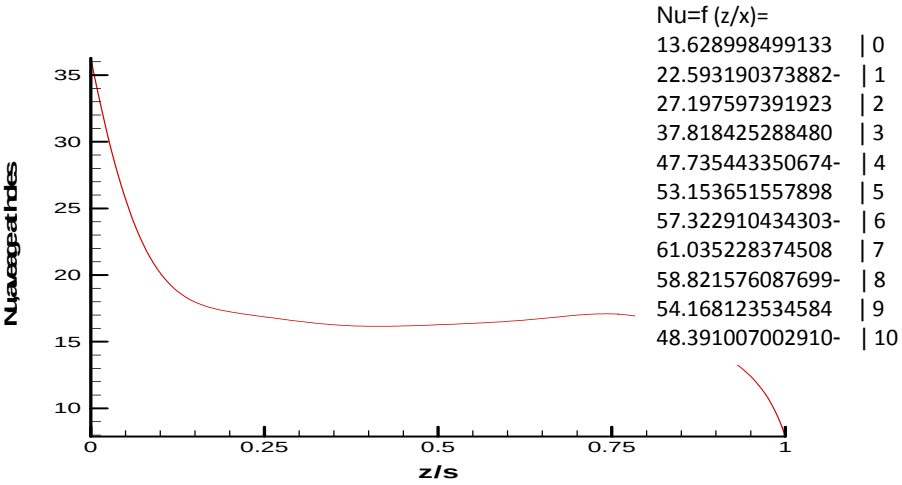

Fig. (9) Nusselt number average in all holes for small tip gap with blowing ratio (1%).

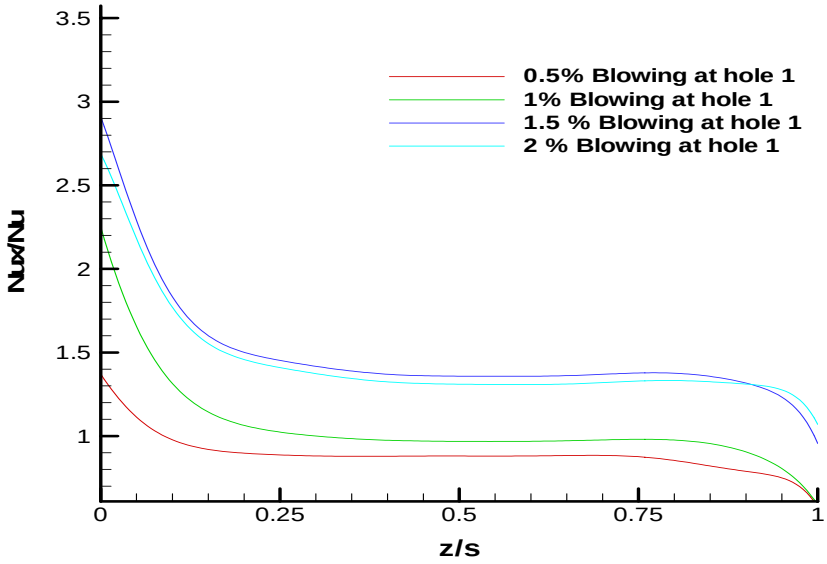

Fig. (10) The Relation between dimensionless Nusselt number and distance of span at different blowing ratio of hole 1.

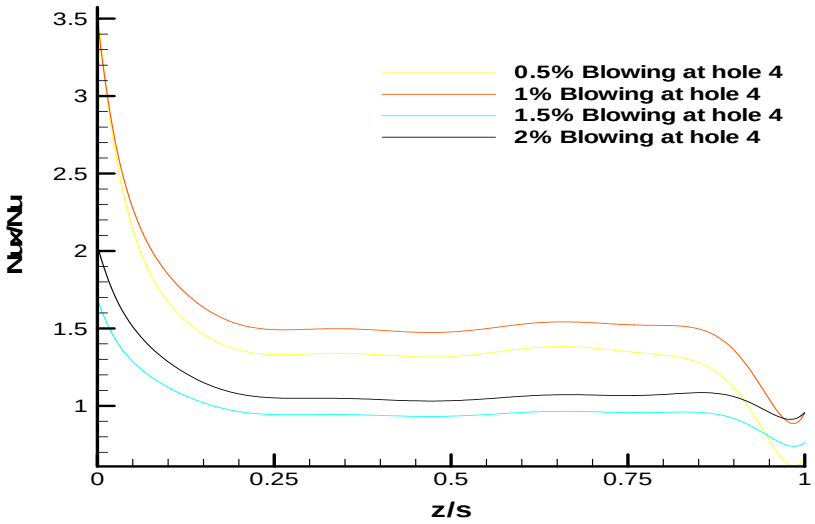

Fig. (11) The Relation between dimensionless nusselt number and distance of span at different blowing ratio of hole 4.